A Phosphine Oxide-Functionalized Cyclam as a Specific Copper(II) Chelator

Marie Le Roy, Simon Héry, Nathalie Saffon-Merceron, Carlos Platas-Iglesias, Thibault Troadec, Raphaël Tripier

A Phosphine Oxide Functionalized Cyclam as a Specific Copper(II) Chelator

Marie M. Le Roy,[a] Simon Héry,[a] Nathalie Saffon-Merceron,[b] Carlos Platas-Iglesias,[c] Thibault Troadec*,[a] and Raphaël Tripier*,[a]

[a] *Univ Brest, UMR CNRS 6521, 6 Avenue Victor Le Gorgeu, 29200 Brest, France.*
** E-mail: thibault.troadec@univ-brest.fr; raphael.tripier@univ-brest.fr*
[b] *Institut de Chimie de Toulouse (UAR 2599), 118 route de Narbonne, 31062 Toulouse Cedex 9, France.*
[c] *Universidade da Coruña, Centro de Investigacións Científicas Avanzadas (CICA) and Departamento de Química, Facultade de Ciencias, 15071, A Coruña, Galicia, Spain*

Abstract

Although cyclam-based ligands are among the strongest copper(II) chelators available, they also usually present good affinity for other divalent cations (Zn(II), Ni(II), Co(II)), with no copper(II)-specific cyclam ligands having been described so far. As such property is highly desirable in a large scope of applications, we present herein two novel phosphine oxide-appended cyclam ligands, that could be efficiently synthesized through Kabachnik-Fields type reactions on protected cyclam precursors. Their copper(II) coordination properties were closely studied by means of different physico-chemical techniques (EPR and UV-Vis spectroscopies, X-ray diffraction, potentiometry). The mono(diphenylphosphine oxide)-functionalized ligand demonstrated a copper(II)-specific behaviour, unprecedented within the cyclam family of ligands. This was evidenced by UV-Vis complexation and competition studies with the parent divalent cations. DFT calculations also confirmed that the particular ligand geometry in the complexes highly favours copper(II) coordination over competing divalent cations, rationalizing the specificity observed experimentally.

Introduction

Copper(II) chelation is a wide field of research owing its importance in a large range of applications, such as ion sensing,[1] catalysis,[2,3] medical imaging radiotracers[4,5] or therapeutic agents,[6,7] amongst others. In such medical applications, where very strong copper-binding is often required, polyazamacrocyclic chelators have emerged as excellent scaffolds, with **cyclam** (1,4,8,11-tetraazatetradecane) in particular showing an impressive affinity for the Cu^{2+} ion (log $K_{[Cu(\mathbf{cyclam})]}$ = 27.2).[8] To further build on the intrinsic properties of the **cyclam** framework, coordinating units have been added through *N*-functionalization, allowing fine tuning of the coordination properties of the ligands towards copper(II) (inertness, complexation kinetics, redox properties, cation selectivity), depending on the targeted application. Copper(II) is considered to be a borderline acid according to Pearson's classification,[9] and thus neutral nitrogen-based coordinating arms have been widely used. However, hard donor groups such as acetate pendants were also introduced (**te2a**$^{2-}$ and **teta**$^{4-}$, Scheme 1), resulting in a clear loss in thermodynamic stability (log K_{LCu} = 21.9 for **teta**$^{4-}$), but a drastic enhancement of the kinetic inertness (robustness in competitive media) of the copper(II) complexes.[10,11] These chelators also provided a first evidence that an optimized number of coordinating atoms for copper(II) (*i.e.* 5 or 6, as in **te2a**$^{2-}$) was more efficient than larger numbers (8 in **teta**$^{4-}$) in terms of inertness and other properties of the complexes for *in vivo* use.[11,12] Among other efficient penta- or hexadentate chelators, mono- and dimethylphosphonate cyclam (**te1p**$^{2-}$ and **te2p**$^{4-}$, Scheme 1) have for instance permitted to reach thermodynamic stability values close to, or higher than, that of the [Cu(**cyclam**)]$^{2+}$ complex (log K_{LCu} = 27.3 and 26.5 respectively for **te1p**$^{2-}$ and **te2p**$^{4-}$), with preserved kinetic inertness.[13,14] Our group also contributed to this field, with the synthesis of mono- and dimethylpicolinate cyclam chelators (**te1pa**$^{-}$ and **te2pa**$^{2-}$, Scheme 1),[15–17] with **te1pa**$^{-}$ providing an enhanced redox stability of the complex, with retained kinetic inertness. Again, the hexadentate **te1pa**$^{-}$ ligand demonstrated better properties than octadentate **te2pa**$^{2-}$ for complex stability, inertness and *in vivo* properties. Recently, we also established that replacing the

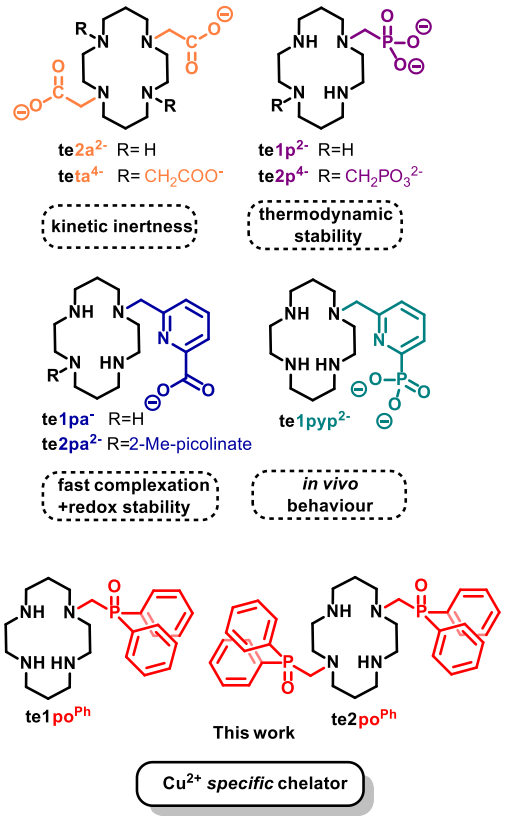

Scheme 1: Copper(II) chelators cited in this work, and **teXpo**^{Ph} ligands (X= 1 or 2) reported herein.

carboxylic acid function of the picolinic group by a phosphonic moiety (**te1pyp**$^{2-}$, Scheme 1) could improve the *in vivo* behaviour of the resulting copper(II) chelate, with lower non-specific fixation and better clearance.[18]

However, while reaching high affinity for copper(II), this series of chelators also demonstrate excellent coordination properties for other biologically relevant metal ions, such as zinc(II), nickel(II) and cobalt(II). Indeed, **teta**$^{4-}$ has very poor selectivity for any of these cations with association constants falling into a four log-units range (from log K_{LM} = 16.7 for Ni^{2+} to 21.9 for Cu^{2+}).[10] The **te1p**$^{2-}$ or **te1pa**$^{-}$ ligands show a dramatically increased affinity for copper(II) (log K_{LCu} = 27.3 and 25.5 respectively), resulting in selectivity for copper(II) versus other metals (*ca.* 7 log units difference in affinity constants), but the affinity for divalent cations is still fairly high (log K_{LZn} = 21.0 and 18.6 respectively),[14,15] not making them specific for copper(II). Such specificity is however highly sought after, for instance in applications such as copper ions sensing[19] or chelation therapy for pathologies such as Alzheimer's disease.[20–22] In these fields, linear ligands are generally preferred, as they maintain sufficient copper association constants (log K_{LCu} ≈ 10-15)[23] as well as a good selectivity over other cations (7 log units or higher), leading to very low affinity values for these ions, and apparent copper(II) specificity. To the best of our knowledge, such specificity is however still elusive in the case of **cyclam** and polyazamacrocycles in general, owing to the excellent match between the macrocyclic cavity and the range of cited divalent cations.

Tertiary phosphine oxides have been used as donor ligands mainly for early transition metals[24,25] and lanthanides.[26] Nevertheless, a few chelating ligands bearing phosphine oxide moieties have been reported for copper(II),[27–30] demonstrating a certain reciprocal affinity. With polyazamacrocycles, to our knowledge, only two examples have been reported so far, namely ethyl- or methyldiphenylphosphoryl tetrasubstituted cyclen,[31,32] for the coordination of alkali metal ions and divalent cations of groups 9-12 respectively, but with no demonstrated selectivity. Thus, we sought to combine the copper(II) coordination properties of both **cyclam** and phosphine oxide sidearms, and we report herein the synthesis of the novel **te1po**^{Ph} ligand and its **te2po**^{Ph} congener. Subsequent coordination chemistry studies were conducted to demonstrate the specificity of **te1po**^{Ph} for copper(II).

Results and Discussion

Synthesis of ligands, complexes and crystal structures. The synthetic protocol for the preparation of the ligands is depicted in Scheme 2, while full experimental details can be found in the experimental section.

The tri(*tert*-butoxycarbonyl)-[33] and *trans*-di(*tert*-butoxycarbonyl)-protected[34] cyclam precursors were reacted with paraformaldehyde and diphenylphosphine oxide in Kabachnik-Fields conditions,[35] leading to Boc-protected functionalized compounds **1** and **2** respectively, with moderate to excellent yields (58-95%). Cleavage of the *tert*-butoxycarbonyl protecting groups with trifluoroacetic acid in dichloromethane, and subsequent precipitation in acetone/aqueous hydrochloric acid solutions afforded the title compounds **te1po**^{Ph} and **te2po**^{Ph} as hydrochloride salts in good yields (60-82%) and with excellent purity (Figures S4-S6 and S11-S13,Supporting Information). Both ligands were fully characterized by multinuclear NMR spectroscopy, exhibiting characteristic ^{31}P NMR chemical shifts (36.5 and 34.4 ppm respectively for **te1po**^{Ph} and **te2po**^{Ph}) for the diphenylphosphoryl moiety. Single crystals of **te2po**^{Ph} could were grown from an ethanolic solution of the ligand and data are presented in Supporting Information (Table S1 and Figure S16)

te1po^{Ph} presents a good solubility in water and thus corresponding [Cu(**te1po**^{Ph})]$^{2+}$ was prepared in aqueous solution with copper(II) perchlorate at pH<6 to avoid any formation of copper hydroxides, leading to the isolation of a purple solid after flash column chromatography (C18-grafted silica). **te2po**^{Ph} demonstrated low solubility in water even when isolated as a hydrochloride salt. Thus, [Cu(**te2po**^{Ph})]$^{2+}$ was prepared in acetonitrile, using the same copper salt, and obtained as a deep blue solid. Single crystals suitable for X-Ray diffraction could be obtained by slow evaporation from saturated methanolic and ethanolic solutions of the [Cu(**te1po**^{Ph})]$^{2+}$ and [Cu(**te2po**^{Ph})]$^{2+}$ complexes, respectively (Figure 1 and Table 1, see collection data in Supporting Information, Tables S2-S3). The structure obtained for [Cu(**te1po**^{Ph})(H_2O)]$^{2+}$ reveals a distorted octahedral geometry around the copper(II) centre, with the four nitrogen donors from the cyclam skeleton occupying the equatorial plane, and the apical positions corresponding to the oxygen atoms from

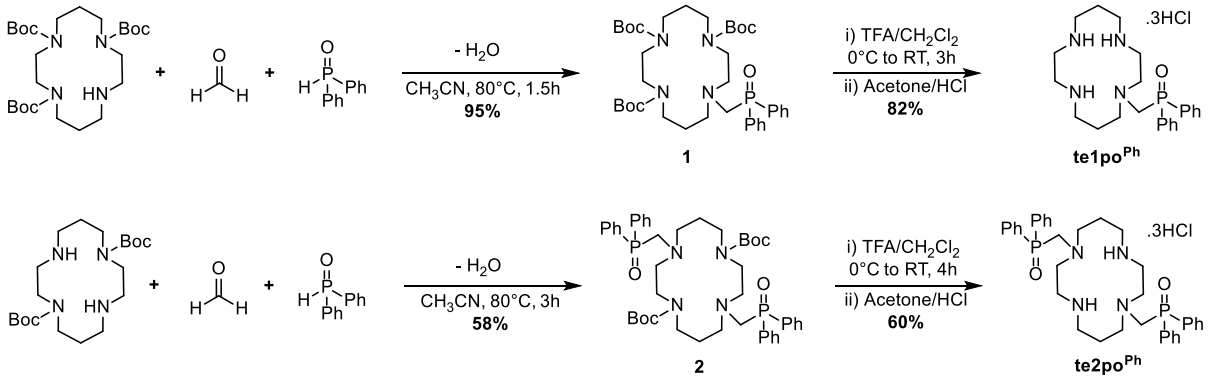

Scheme 2: Synthesis of ligands **te1po**^{Ph} and **te2po**^{Ph}

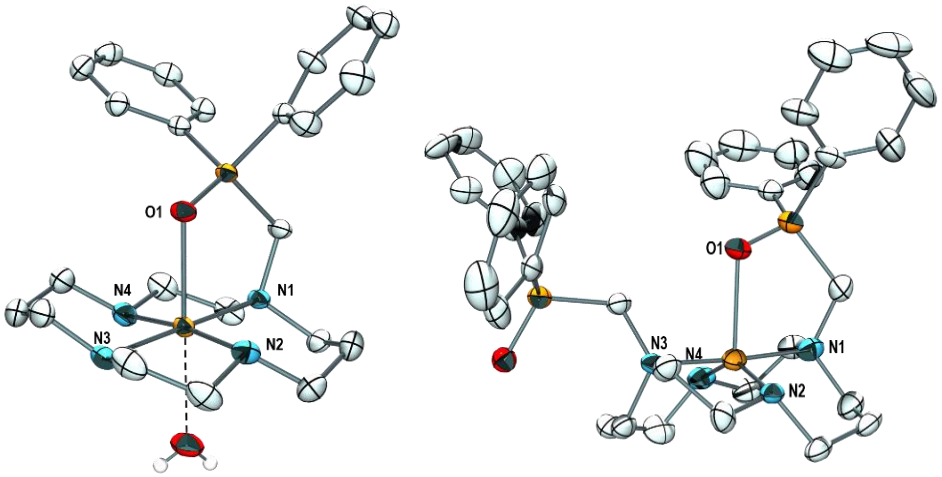

Figure 1: X-Ray diffraction structures of complexes [Cu(**te1po^{Ph}**)(H_2O)]$^{2+}$ (left) and [Cu(**te2po^{Ph}**)]$^{2+}$ (right). Ellipsoids drawn at 50% probability. H atoms, anions and solvent molecules are omitted for clarity (except coordinated water in [Cu(**te1po^{Ph}**)(H_2O)]$^{2+}$).

Table 1: Selected Bond distances (Å) and angles (°) observed in the crystal structures of [Cu(te1po^{Ph})(H_2O)]$^{2+}$ and [Cu(te2po^{Ph})]$^{2+}$.

	Cu-N	Cu-Cnt‡	Cu-O	P-O-Cu
[Cu(**te1po^{Ph}**)(H_2O)]$^{2+}$	2.08(N1)	0.07	2.36 *(P-O)*	109.3(1)
	2.01(N2)		2.52 *(H_2O)*	
	2.03(N3)			
	2.02(N4)			
Cu(te2po^{Ph})$^{2+}$	2.05(N1)	0.23†	2.25†	111.0(2)
	2.00(N2)			
	2.06(N3)			
	2.01(N4)			

‡ Cnt = N1-N2-N3-N4 calculated centroid; † average value of the 3 molecules in asymmetric unit. Error in parenthesis for angles. Error < 0.01Å for bond distances (Supporting Information, tables S2-S3).

the phosphoryl fragment and a water molecule. Among its six possible conformations,[36] the macrocycle adopts here the *trans*-III geometry, which is one of the most stable conformations for cyclam derivatives in their Cu^{2+} complexes,[37] and was observed for instance for the complex with the pentadentate **te1p** ligand.[14] The arrangement of the four nitrogen atoms around the metal is nearly planar, with the bond involving the tertiary amine (Cu-N1) being only slightly longer than the remaining three (2.08 Å *vs* 2.00-2.03 Å for N2-4)). The copper(II) centre deviates only by 0.07 Å from the centroid defined by N1, N2, N3 and N4. The Cu-O1 distance (2.36 Å) is in the range of the few previously described apical phosphine oxide ligands in octahedral copper(II) (2.31 to 2.44 Å),[30] and anionic phosphonate moieties in Cu(Hte1p)Br and Cu(H_2te2p) complexes (2.37 and 2.31 Å respectively).[13,14] This similarity with phosphonates can be rationalized by the peculiar bonding situation of the P-O fragment in phosphine oxides,[38,39] that is far from the formally neutral double-bond, but is best described with a highly polarized σ–bond component and high electron density on the oxygen atom. However, the rather unusual feature observed in this structure is the very small P-O1-Cu angle (109.3°), which is imposed by the topology of the ligand, and is in marked contrast with the usual linear orientation of phosphine oxide fragments in coordination compounds (P-O-M angle tending towards 180°), which minimizes electrostatic repulsion between the electropositive cation and phosphorus atom.[26]

The crystal structure of [Cu(**te2po^{Ph}**)]$^{2+}$ presents three independent molecules of the complex, with very similar angles and bond lengths, within the asymmetric unit. These reveal a five-coordinate square pyramidal copper centre, despite the presence of the additional phosphine oxide coordinating group. This feature has already been observed with parent hexadentate **te2p^{4-}**,[13] and can be explained by the differentiation of the four N-donors into two secondary and two tertiary amines, which display different steric demand and thus different bond lengths with copper (2.06 and 2.05 Å for tertiary *vs* 2.00 and 2.01 Å for secondary). This results in a *trans*-I complex conformation, with both 6-membered chelate rings pointing in the same direction, and the copper ion being placed markedly above the basal plane formed by the four nitrogen donors (0.23 Å distance between the Cu^{2+} ion and the centroid defined by N1-N2-N3-N4). The Cu-O bond with the phosphoryl moiety is thus accordingly shortened (2.25 Å vs. 2.36 Å in [Cu(**te1po^{Ph}**)(H_2O)]$^{2+}$, with the P-O-Cu angle maintained to a similar value (111.0° vs. 109.3°).

Solution-state properties. To gain insight in the solution structure of these paramagnetic complexes, electron paramagnetic resonance measurements were conducted with frozen dimethylformamide/water (1:1) solutions (150 K, X-band, Figure 2). Simulated spectra were then generated (Easyspin/Simultispin software suite)[40,41] to obtain the corresponding $g_{x,y,z}$ and $A_{x,y,z}$ parameters (Table 2). Both complexes present *g* values ($g_x \approx g_y < g_z$) corresponding to a $d_{x^2-y^2}$ ground state, which is compatible with the axial symmetry of the elongated octahedral and square pyramidal geometries observed in the solid-state structures of [Cu(**te1po^{Ph}**)(H_2O)]$^{2+}$ and [Cu(**te2po^{Ph}**)] respectively. The value of A_z is clearly higher

for [Cu(**te1po^{Ph}**)]$^{2+}$ than for [Cu(**te2po^{Ph}**)]$^{2+}$, which suggests that these complexes maintain in solution the respective *trans*-III and *trans*-I conformations observed in the solid state. Indeed, the values of A_z fall slightly below the ranges that characterize *trans*-III ((195-210)×10^4 cm^{-1}) and *trans*-I ((181-195)×10^4 cm^{-1}) respectively. Furthermore, the values of $g_z + |g_y - g_x|$ of 2.20 and 2.22 obtained for [Cu(**te1po^{Ph}**)]$^{2+}$ and [Cu(**te2po^{Ph}**)]$^{2+}$ fall within the ranges observed previously for *trans*-III and *trans*-I isomers.[42]

The *g*- and *A*-tensors of [Cu(**te1po^{Ph}**)]$^{2+}$were also computed using DFT calculations, using the optimized geometries of the *trans*-III and *trans*-I isomers. Unfortunately, the theoretical calculation of *g*- and *A*-tensors with DFT is rather difficult, with the results obtained being highly dependent on the functional used. Furthermore, we are not aware of a functional capable of providing accurate results for both *g*- and *A*-tensors. Herein, we used the TPSSh functional for the calculation of *A*-tensors, following previous work reported by us and others.[42,43] The *g*-tensors were obtained with scalar relativistic calculations using double hybrid DFT with the PBE0-DH functional (see computational details below), using the methodology proposed very recently by Pantazis.[44] The EPR parameters calculated for the *trans*-III isomer show an excellent agreement with the experimental data recorded for [Cu(**te1po^{Ph}**)]$^{2+}$, while those obtained for the *trans*-I isomer are closer to those measured for [Cu(**te2po^{Ph}**)]$^{2+}$ (Table 2). In particular, the *trans*-III isomer is characterised by a slightly lower g_z value and a higher A_z value. These results confirm that [Cu(**te1po^{Ph}**)]$^{2+}$and [Cu(**te2po^{Ph}**)]$^{2+}$ are present in solution as the *trans*-III and *trans*-I isomers, respectively.

Owing to the poor solubility of **te2po^{Ph}** ligand in aqueous media, all further experiments were conducted on **te1po^{Ph}** only. In these experiments, the [Cu(**te1po^{Ph}**)]$^{2+}$ complex was prepared at 25°C from equimolar mixtures of **te1po^{Ph}** ligand and Cu^{2+} cation (2 mM), and the structure of the complex was unambiguously confirmed by EPR spectroscopy as identical to the one prepared in refluxing aqueous solution (Figure S19, Supporting Information). Thermodynamic studies by means of potentiometric titrations were undertaken to determine the protonation constants of the ligand and complex stability constants. Among the four possible protonation events (on the four basic amines of the cyclam scaffold), only three could be accurately determined with our experimental conditions ([**te1po^{Ph}**] ≈ 1.6mM in 0.1M K(NO_3) at 25°C), the fourth being too low and out of the pH range useful for pH potentiometric measurements (1.5-11.5). As usually observed for cyclam derivatives, two strongly basic amines (in *trans* position within the macrocyclic ring) are characterised by two protonation constants with log K_{11} and log K_{12} values generally above 9. The third protonation event is usually much more difficult owing to the electrostatic repulsion generated by the presence of a third ammonium group within the macrocyclic cavity. The **te1po^{Ph}** ligand follows this trend, although the first two constants (log K_{11} = 10.68 and logK_{12} = 8.98) are substantially lower than those observed for other monosubstituted cyclam analogues (Table 3). This lower overall basicity of **te1po^{Ph}** is evidenced by looking at the sum of these first two constants (log K_{11} + log K_{12} = 19.66

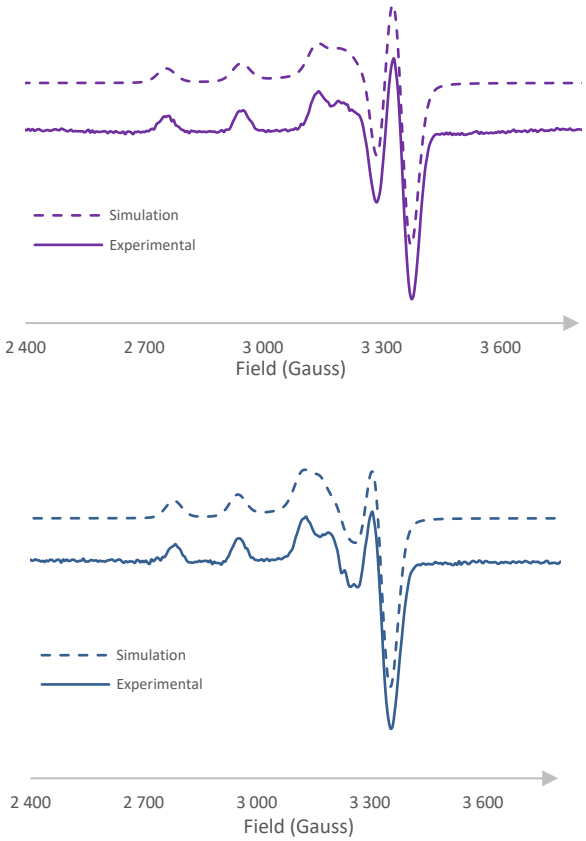

Figure 2: X-band EPR spectrum of copper(II) complexes **Cu(te1po^{Ph})(H$_2$0)$^{2+}$** (top, – experimental; - - - simulation) and **Cu(te2po^{Ph})$^{2+}$** (bottom, – experimental; - - - simulation) recorded in frozen aqueous solution (1:1 DMF/H2O, 1.0 mM; 150K).

Table 2: Calculated parameters from EPR measurements performed in 1:1 H_2O/DMF glass (1.0 mM, 150 K; Ai values quoted in 10^{-4} cm^{-1})

	g_x	g_y	g_z	A_x	A_y	A_z
[Cu(te1po^{Ph})]$^{2+}$	2.04	2.03	2.19	1.23	39.14	194.08
[Cu(te2po^{Ph})]$^{2+}$	2.06	2.04	2.20	1.70	52.74	174.67

for **te1po^{Ph}**), which is more than 2 log units lower than those of ligands bearing anionic arms (log K_{11} + log K_{12} = 24.25 for **te1p^{2-}** and 21.66 for **te1pa**). However, the basicity of **te1po^{Ph}** is closer to that of **te1EtOH** (20.68), bearing a neutral hydroxyethyl arm. As global basicity of these ligands is closely related to their coordinating ability towards metal cations, potentiometric titrations in the presence of Cu^{2+} cations were carried out. Unfortunately, in our experimental conditions ([**te1po^{Ph}**] = 1.61 mM in 0.1M KNO_3, 25°C), precipitation of hydroxide species (of copper or the **te1po^{Ph}** complex) occurred above pH = 7.5, preventing accurate data collection on the whole pH range. The stability constant of the new ligand could nevertheless be estimated using data from the 1.5-7.5 pH range (calculated log K_{LCu} = 17.8(1)). To further corroborate this value, a fixed-pH UV-Vis titration was conducted (batch titration, pH = 3.0, from 0.2 to 2.0 equiv. Cu^{2+}), confirming the range of the estimated value

Table 3. Protonation and cation complexation constants (log *K*) for **te1po^{Ph}** and closely related systems reported in the literature.

log K_{lh} (± 3σ)					
Constant[a]	**te1po^{Ph}**	**te1p**[b]	**te1pa**[c]	**te1EtOH**[d]	**Cyclam**[e]
log K_{11}	10.68(6)	12.49	11.55	10.93	11.29
log K_{12}	8.98(8)	11.76	10.11	9.75	10.19
(log K_{11} + log K_{12})	19.66	24.25	21.66	20.68	21.48
log K_{13}	1.63(8)	*(6.05)*‡	*(2.71)*†	1.66	1.61
log K_{14}	< 1.5	*(2.42)*‡	1.7		1.91
log K_{15}		< 1.5			
log K_{lm} (± 3σ)					
log K_{LCu}	17.8 (1)[f] 18.5 (1)[g]	27.3	25.5	16.6	28.1
log K_{LZn}	-	21.0	18.9	10.3	15.0

[a] Stepwise protonation constants log K_{lh} correspond to equilibria $LH_{(h-1)} + H \leftrightarrows LH_h$ / Association constants log K_{lm} correspond to equilibria $L + M \leftrightarrows LM$; [b]Ref 13; [c] Ref 15; [d] Ref 46; [e] Ref 45; [f] Determined by potentiometry (1.5 – 7.5 pH range); [g] Determined by UV-Vis titration at fixed pH (pH = 3).
‡ Phosphonate group; † Acetate group.

(log K_{LCu} = 18.5(1)) with this technique. As expected when discussing the basicity of the ligand, this copper(II) affinity is much lower than the one of parent **cyclam** and monosubstituted analogues (log K_{LCu} > 25 for **cyclam**,[45] **te1p^{2-}** and **te1pa^{-}**, Table 3), and in the range of its neutral te1EtOH congener (log K_{LCu} = 16.6).[46] The kinetic inertness of the [Cu(**te1po^{Ph}**)]$^{2+}$ complex was also examined, through acid-assisted dissociation under pseudo-first order conditions in excess HCl solution at 25.0 °C. This type of experiment provides good insight on the robustness of the macrocyclic complexes towards dissociation in highly competitive media (as ligands are strongly basic). The dissociation of the complex was monitored by UV-Vis spectroscopy, with the decrease of the characteristic d–d absorption band at 550 nm (Figure S20, Supporting Information). The obtained half-life values of 10 hours in 1M HCl and 5.6 hours in 5M HCl demonstrated that the complex is sufficiently inert for many applications, and even more inert than the previously described [Cu(**te1pa**)]$^{+}$ (32 min in 1M HCl at 25°C),[15] which is highly inert *in vivo*.[47] The evolution of the complex in basic conditions, evidenced in potentiometric titrations (*vide supra*), was also confirmed by UV-Vis monitoring of a solution of the complex in water at pH 8.5 (adjusted with KOH). A half-life of 50 minutes was calculated in these conditions (Figure S21, Supporting Information), with again the observation of a grey precipitate, which could be isolated from the supernatant but could unfortunately not be redissolved at lower pH to identify its actual nature. However, the stability of the complex was investigated at physiological pH in TRIS buffer (pH 7.3), showing no dissociation after up to 30 hours at 25°C (Figure S22, Supporting Information).

When it comes to other divalent cations, interestingly, potentiometric titrations of **te1po^{Ph}** in presence of zinc(II) cations in the 2 – 11.5 pH range did not reveal formation of the corresponding complex. Synthesis was also attempted with equimolar mixtures of ligand and zinc(II) in refluxing water or acetonitrile, but no complex formation could be identified by NMR spectroscopy or mass spectrometry. To further assess this potential copper(II)-specificity, complexation studies were performed with other divalent cations as well.

UV-Vis complexation and competition studies. Zinc(II), nickel(II) and cobalt(II) were selected for these studies, owing to their common affinity for cyclam-based ligands. Measurements were conducted in aqueous acetate buffer (pH = 3.8), with a ligand concentration of 2 mM. As the free cations can interact with acetate anions in solution, providing signals on the 200-800 nm range (Figure S23, Supporting Information), all spectra presented here were background-corrected with solutions of the corresponding free cations in the same buffer. All samples were equilibrated for 48h at 25°C prior to data collection, to avoid the possible effect of different complexation kinetics of the ligand with the different cations. First, individual equimolar mixtures of **te1po^{Ph}** with each of the four cations were analysed (Figure 3a). Copper(II) complex formation is clearly observed thank to the band at λ = 579 nm, characteristic of the copper(II)-centered d-d electronic transition in such distorted octahedral geometry.[48] On the other hand, the spectra recorded in the presence of Zn^{2+}, Ni^{2+} and Co^{2+} indicate that no complexation takes place, as evidenced by the perfect overlap with the spectrum of free **te1po^{Ph}** ligand. To highlight this impressive specificity for copper(II), further competition experiments were carried out. First, **te1po^{Ph}** was incubated with an equimolar amount of Cu^{2+} and an excess (5.0 equiv.) of each of the competing cations in separate experiments (Figure S24, Supporting Information). Unambiguously, in each case, the spectrum overlaps with the one of the in situ generated [Cu(**te1po^{Ph}**)]$^{2+}$ complex. The cobalt(II) and nickel(II) samples exhibit slight deviations around 600 and 400 nm, but these could be attributed to background noise from the absorption of free cobalt(II) and nickel(II) ions in acetate buffer (Figure S23, Supporting Information), and not to complexation of these cations by the ligand. Experiments with greater excess of these two competing cations could not be carried out, as the d-d transition bands of the copper complex would be masked by absorption bands of the free cations at higher concentration. However, the study with 100 equiv. of Zn^{2+} was performed, and confirmed again the very high selectivity of the ligand for copper (Figure 3b). This striking specificity of **te1po^{Ph}** for copper was finally confirmed through mixed competition experiments where the ligand was incubated with equimolar amounts of each cation in the same sample at pH 3.8 (Figure S24, Supporting Information), and up to a 5-fold excess of each cation at pH 7.3 in TRIS buffer (Figure 3c). Even though a small deviation is observed in the last case, it can be again confidently attributed to the background noise of the free cations in the solution, and in both cases, only the copper(II) complex is formed, as demonstrated by the overlap of the sample spectrum with the one of the in situ generated [Cu(**te1po^{Ph}**)]$^{2+}$ complex.

The stability trend of the [M(**te1po^{Ph}**)]$^{2+}$ complexes (M = Co, Ni, Zn) was further analysed with DFT by computing the Gibbs free energies for the following reaction (M = Co, Ni or Zn):[49]

$$[Cu(H_2O)_6]^{2+} + [M(\textbf{te1po}^{Ph})]^{2+} \leftrightarrows [M(H_2O)_6]^{2+} + [Cu(\textbf{te1po}^{Ph})]^{2+} \quad (1)$$

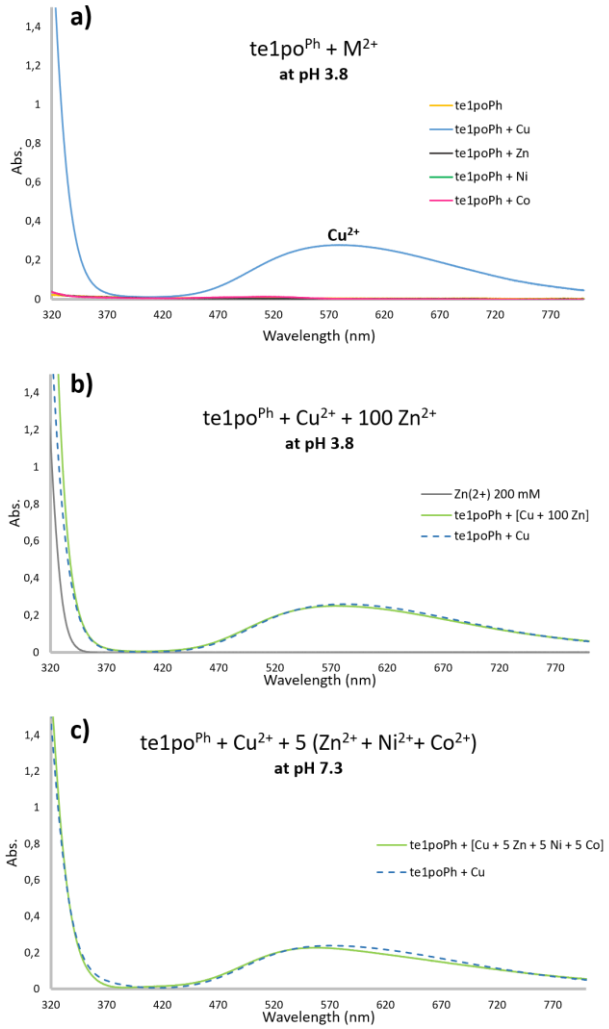

Figure 3: UV-Vis complexation and competition experiments. Conditions : 25°C, [**te1po^{Ph}**] = 2mM. a) Individual cation complexation in acetate buffer (pH 3.8) : ([M^{2+}] = [**te1po^{Ph}**] = 2mM; b) Competition in acetate buffer (pH 3.8), [Cu^{2+}] = [**te1po^{Ph}**] = 2mM, [Zn^{2+}] = 200mM; c) Mixed competition in TRIS buffer (pH 7.3), [Cu^{2+}] = [**te1po^{Ph}**] = 2mM, [M^{2+}] = 10mM.

For these calculations, we carried out geometry optimizations of the [M(**te1po^{Ph}**)]$^{2+}$·H_2O systems at the wB97XD/Def2-TZVPP level, which yielded *trans*-III minimum energy conformations for M = Cu and Ni, and *trans*-I conformation for M = Co and Zn (Tables S4-S7 and Figure S25, Supporting Information). For the aquo-complexes, we performed calculations on the [M(H_2O)$_6$]$^{2+}$·12H_2O systems, which incorporate 12 explicit second-sphere water molecules (Tables S8-S11 and Figure S26, Supporting Information).[50,51] This allowed to overcome the known convergence problems faced when optimizing the [M(H_2O)$_6$]$^{2+}$ systems using polarized continuum models.[52] Our DFT calculations afford $\Delta G°$ values of -76, -52 and -46 kJ mol^{-1} for M = Co, Ni and Zn, respectively. This is in line with the Irving-Williams order, which predicts a trend in complex stability such that Co^{2+} < Ni^{2+} < Cu^{2+} > Zn^{2+}. These free energy differences correspond to log*K* values in the range 8.1-13.3. While these DFT estimates have to be taken with some care, they support an impressive selectivity of the ligand for 8 Cu^{2+} over Co^{2+}, Ni^{2+} and Zn^{2+}. A stability constant of log K_{CuL} = 8 implies that complex dissociation is almost complete below pH 5, while for log K_{ML} =13 full dissociation takes place below pH ~3.0 (at 1 mM metal and ligand concentrations).The reasons for the observed specificity appear to be related to the presence of the bulky diphenylphosphine oxide pendant arm, which likely introduces certain steric hindrance for metal ion coordination. This steric hindrance is alleviated in the case of Cu^{2+} due to the long axial distance associated to the Jahn-Teller effect (2.214 Å for [Cu(**te1po^{Ph}**)]$^{2+}$ versus 2.100 Å in [Zn(**te1po^{Ph}**)]$^{2+}$).

Conclusion

Two new cyclam-based ligands with diphenylphosphine oxide pendants were prepared, and their corresponding copper(II) complexes were isolated and characterized. As the solubility of the disubstituted **te2po^{Ph}** ligand is low in aqueous media, only the coordination properties of the monosubstituted **te1po^{Ph}** analogue were fully investigated. In particular, potentiometric and UV-Vis titrations allowed to evaluate thermodynamic constants of the ligand, revealing a much lower global basicity and copper association constant (log $K \approx 18$) when compared to the strongest copper(II) chelators of the family (picolinate and methylphosphonate analogues, log $K > 25$). However, this decrease is combined with a strong diminution in affinity for other divalent metal ions, that could not be measured experimentally but was estimated by DFT calculations. This results in an impressive specificity for copper(II), evidenced through competition titration experiments carried in water at room temperature at acidic (pH 3.8) or at physiological pH. Although the stability of the complex in basic conditions could be enhance in future ligand modifications, this model proved stable around physiological pH. Therefore, **te1po^{Ph}** presents a rare example of copper(II)-specificity, and is the first member of the cyclam family demonstrating such behaviour. Various fields where this feature is a crucial parameter (ion sensing, chelation therapy) could be explored in the future as interesting applications for this novel azamacrocyclic chelator.

Experimental Section

Materials & Methods. Reagents were purchased from Sigma-Aldrich®, TCI Chemicals®, Acros Organics®, Ultrapure water was freshly obtained from a Milli-Q dispenser. Triboc-cyclam and diboc-cyclam were synthesized as previously described.[33,34] NMR data were recorded at the "Service commun de RMN-RPE" at the Université de Bretagne Occidentale (UBO). ^{1}H, ^{13}C and 2D NMR spectra were recorded on Bruker Avance III HD 500 (500.25 MHz for ^{1}H and 125.79 MHz for ^{13}C), Bruker Avance 400 (400.13 MHz for ^{1}H and 100.62 MHz for ^{13}C) or Bruker AMX-3 300 (300.13 MHz for ^{1}H and 75.47 MHz for ^{13}C) spectrometers. All ^{31}P and ^{13}C spectra are proton decoupled unless otherwise stated. High Resolution Mass Spectrometry (HRMS) spectra

were recorded at the HRMS platform of the University of Orleans, France (FR 2708 CBM-ICOA).

Analytical HPLC. Measures were performed on a Prominence Shimadzu HPLC/LCMS-2020 instrument equipped with an UV SPD-20 A detector. The chromatographic system employs C18AQ 5 µM 250 × 4.6 mm columns with H_2O (0.1% TFA) – MeCN or MeOH (v/v) as eluents at a flow rate of 1 mL/min and UV detection at 254 and 350 nm.

Electron Paramagnetic Resonance Studies. Spectra were recorded at the "Service Commun de RMN-RPE" at the Université de Bretagne Occidentale (UBO) on a Bruker Elexsys 500 instrument, in a 0.5 mm capillary within a quartz tube, at 9.34 GHz (band X) using a complex concentration of ca. 1.0 mM. Simulations of the experimental spectra were performed using Easyspin[53] and Simultispin[54] software.

UV-Vis and Kinetic Inertness Studies. UV-Vis spectra were recorded at 25°C on a JASCO V-760 spectrometer equipped with a PAC-743R Peltier temperature control device. UV-Vis apparatus in 700 μL cuvettes with 1 cm optical path, and a baseline correction was applied. Acid- and base-assisted dissociation experiments were carried out with a complex concentration of 4mM. Stability in TRIS buffer was conducted at a complex concentration of 2mM

X-Ray Diffraction Analysis. Crystallographic data collection was performed at low temperature (193 K) at the Service RX of the Institut de Chimie de Toulouse, Université Paul Sabatier, on a Bruker-AXS APEX II CCD diffractometer equipped with a 30 W air-cooled microfocus source for [Cu(**te2po^{Ph}**)]$^{2+}$ or on a Bruker-AXS D8-Venture diffractometer for **te2po^{Ph}** ligand and [Cu(**te1po^{Ph}**)(H_2O)]$^{2+}$ using MoKα radiation (λ = 0.71073 Å). Phi- and omega-scans were used. The data were integrated with SAINT (Program for data reduction, Bruker-AXS) and an empirical absorption correction with SADABS was applied (Program for data correction, Bruker-AXS). The structures were solved using an intrinsic phasing method (ShelXT)[55] and refined using a least-squares method on F^2.[56] All non-H atoms were refined with anisotropic displacement parameters. Hydrogen atoms were refined isotropically at calculed positions using a riding model except H atoms on nitrogen and water molecules (located by difference Fourier maps). Some parts of the complex [Cu(**te2po^{Ph}**)]$^{2+}$ and the ligand **te2po^{Ph}** were found to be disordered. Several restraints (SAME, SIMU, DELU, SADI, ISOR, DFIX) and equal xyz and U_{ij} constraints (EXYZ and EADP) were applied to refine some moieties of the molecules and to avoid the collapse of the structures during the least-squares refinement by the large anisotropic displacement parameters.

For complex [Cu(**te2po^{Ph}**)]$^{2+}$, some residual electron density was difficult to modelize and therefore, the SQUEEZE function of PLATON[57] was used to eliminate the contribution of the electron density in the solvent region from the intensity data, and the solvent-free model was employed for the final refinement. CCDC 2237998 (**te2po^{Ph}** ligand), 2237999 ([Cu(**te1po^{Ph}**)(H_2O)]$^{2+}$) and 2238000 ([Cu(**te2po^{Ph}**)]$^{2+}$) contain the supplementary crystallographic data for this paper. These data can be obtained free of charge from The Cambridge Crystallographic Data Centre via https://www.ccdc.cam.ac.uk/structures/.

Computational details. Geometry optimizations and frequency calculations werte performed with the Gaussian16 program package[58] using the wB97XD[59] functional and the Def2-TZVPP[60] basis set for all atoms. Solvent effects were incorporated using a polarized continuum model[61] with the default parameters implemented in Gaussian [scrf=(pcm,solvent=water)]. The structures of the $[M(H_2O)_6]^{2+}\cdot 12H_2O$ systems were optimized using input structures from previous computational studies.

The ^{63}Cu hyperfine coupling tensors and *g* tensors were calculated with the ORCA program package (version 5.0.3).[62,63] Hyperfine coupling constants were obtained using DFT with the TPSSh functional[64] and the Def2-QZVPP[60] basis set. TPSSh was found to yield good results for both organic radicals and metal complexes.[43] The calculation of *g*-tensors was performed using the double hybrid PBE0-DH functional,[65] including scalar relativistic effects with the ZORA approximation,[66,67] using the def2-TZVPP basis set recontracted for ZORA calculations for Cu and ZORA-def2-TZVP for ligand atoms.[60,68] All calculations were accelerated using the resolution of identity and chain-of-spheres (RIJCOSX) approximation[69] with auxiliary basis sets obtained with the Autoaux procedure.[70] Spin-orbit coupling (SOC) contributions were considered using the spin-orbit mean-field (SOMF(1X)) method.[71,72] All ORCA calculations incorporated water solvent effects with the SMD solvation model.[73]

Potentiometric measurements. The potentiometric titrations of the free ligand **te1po^{Ph}** (1.61×10^{-3} M) and complex formation ($[M(II)]_{tot}$ = 0.95 $[$**te1po^{Ph}**$]_{tot}$) were performed using an automatic titrator system 794 Basic Titrino (Metrohm) with a combined glass electrode (Metrohm 6.0234.500, Long Life)

$$U = \sum_{i}^{N} W_i (E_{obs,i} - E_{cal,i})^2$$

filled with 0.1 M KCl in water and connected to a computer (Tiamo light 1.2 program). The ionic strength of the solutions was kept at 0.10 ± 0.01 M with KNO_3. The temperature of the titration cell was maintained at 25.0 ± 0.2 °C with the help of a Lauda E200 thermostat. KOH solution was prepared just before use from Fixanal® cartridges, and its accurate concentration was obtained through the application of the Gran method upon the titration of a standard HNO_3 solution. Glass electrode calibration was achieved before every titration with Glee software[74] to calculate electrode parameters (standard electrode potential E_0[mV] and slope [mV.pH^{-1}]) and to check carbonate levels of the KOH solutions used (< 5 %). Each in-cell titration consisted of 70-120 equilibrium points in the range pH 2.0-11.5, and at least three replicate titrations were performed for each particular system. Data were analyzed with Hyperquad 2008 software,[75] with non-linear least-squares methods.[76] The constants were refined by minimizing the error-square sum, U, of the potentials:

The three potentiometric titrations were treated as a single set for the protonation of **te1po^{Ph}**. The association and stepwise protonation constants (log K) were calculated from the overall constants (log β) obtained with the software. The uncertainties in the log K values correspond to the added standard deviations in the overall constants. The Cu^{2+} and Zn^{2+} solutions were prepared at ca. 0,05 M from analytical-grade nitrate salts and

standardized by complexometric titrations with ethylenediaminetetraacetic acid (H_4edta)

***Synthetic procedures*.**

Synthesis of 1: Under nitrogen, triboc-cyclam (0.604 g, 1.21 mmol), diphenylphosphine oxide (0.245 g, 1.21 mmol) and paraformaldehyde (0.036 g, 1.21 mmol) were solubilized in dry CH_3CN (2 mL). The reaction was stirred at 80°C for 1h30. Solvents were removed in vacuo. The crude product was purified by column chromatography on silica gel (100:0 to 96:4 DCM/MeOH) to give **1** as a white foam (0.824 g, 95%).

^{1}H NMR (CD_3CN, 500 MHz, 343 K, TMS) δ (ppm) 7.85-7.79 (m, 4H, CH_{Ar}), 7.59-7.50 (m, 6H, CH_{Ar}), 3.42 (d, 2H, N-CH_2-PO, $^2J_{H-P}$ = 5.3 Hz), 3.24-3.05 (m, 12H, C$H_2\alpha$N), 2.79-2.71 (m, 4H, C$H_2\alpha$N), 1.68-1.55 (br, 4H, C$H_2\beta$N), 1.44 (s, 28H, CH_3Boc). *^{13}C NMR* (CD_3CN, 125 MHz, 343 K, TMS) δ (ppm) [156.8, 156.6, 156.5] (*C*O-Boc), 135.1 (d, C_{ipso}, $^1J_{C-P}$ = 94.8 Hz), 132.9 (*C*H$_{Ar}$), 132.3 (d, *C*H$_{Ar}$, $^2J_{C-P}$ = 8.8 Hz), 129.8 (d, *C*H$_{Ar}$, $^3J_{C-P}$ = 13.2 Hz), [80.2 (x2), 80.1] (C_{sp}-Boc), 57.0, 56.9, 56.8, 56.3, 55.3, 55.2,[48.3, 48.0, 47.8, 47.6, 47.0] (*C*H$_2\alpha$N), 29.9 (*C*H$_2\beta$N), 29.1 (*C*H$_3$-Boc), 27.7 (*C*H$_2\beta$N). *^{31}P NMR* (CD_3CN, 202 MHz, 343 K, H_3PO_4) δ (ppm) 27.0 (*P*=O). *ESI-HR-MS* (positive, H_2O) *m/z* calcd. for $[C_{38}H_{60}N_4O_7P]^+$,715.4194 found $[M+H]^+$ 715.4198, calcd. for $[C_{38}H_{59}N_4NaO_7P]^+$ 737.4014, found $[M+Na]^+$ 737.4010, calcd. for $[C_{26}H_{49}N_4O_6]^+$ 513.3647 found $[M+H\text{-}POPh_2]^+$.

Synthesis of* te1po^{Ph}*: Compound **1** (0.824 g, 1.15 mmol) was dissolved in dichloromethane (7 mL) and trifluoroacetic acid (7 mL) was added at 0°C. The resulting mixture was stirred for 3 h at RT. The reaction mixture was concentrated in vacuo, dissolved in NaOH (4M) and extracted with CH_2Cl_2 (3 x 15 mL). The organic phase was dried over $MgSO_4$, filtered, and concentrated. The product was dissolved with minimal HCl (3M), then acetone was added, and the precipitate was isolated by cannula-filtration to afford **te1po^{Ph}** as a white powder (0.493 g, 82 %). *^{1}H NMR* (D_2O, 400 MHz, 298 K, TMS) δ (ppm) 7.88-7.80 (m, 4H, CH_{Ar}), 7.75-7.59 (m, 6H, CH_{Ar}), 3.83 (d, 2H, CH_2, $^2J_{H-P}$ = 3.4 Hz), 3.44-3.21 (m, 8H, C$H_2\alpha$N), 3.14-3.07 (m, 2H, C$H_2\alpha$N), 3.00-2.95 (m, 2H, C$H_2\alpha$N), 2.75-2.68 (br, 2H, C$H_2\alpha$N), 2.43-2.27 (br, 2H, C$H_2\alpha$N), 2.27-2.13 (br, 2H, C$H_2\beta$N), 1.77-1.61 (br, 2H, C$H_2\beta$N). *^{13}C NMR* (D_2O, 125 MHz, 298 K, TMS) δ (ppm) 136.3 (*C*H$_{Ar}$), 133.6 (d, *C*H$_{Ar}$, $^2J_{C-P}$ = 9.6 Hz), 132.2 (d, *C*HAr, $^2J_{C-P}$ = 11.5 Hz), 131.4 (d, C_{ipso}, $^1J_{C-P}$ = 98.7 Hz), 57.7 (*C*H$_2\alpha$N), 55.0 (d, NCH$_2$P, $^1J_{C-P}$ = 88.7 Hz), 52.3 (d, *C*H$_2\alpha$N, $^3J_{C-P}$ = 6.6 Hz), [45.8, 44.9, 44.2, 44.1, 42.9, 40.6] (*C*H$_2\alpha$N), [25.1, 23.4] (*C*H$_2\beta$N), [25.1, 23.4] (*C*H$_2\beta$N). *^{31}P NMR* (D_2O, 162 MHz, 298 K, H_3PO_4) δ (ppm) 36.5 (*P*=O). *ESI-HR-MS* (positive, H_2O) *m/z* calcd. for $[C_{23}H_{36}N_4OP]^+$415.2621 found $[M+H]^+$ 415.2626, calcd. for $[C_{23}H_{35}N_4NaOP]^+$ 437.2441 found $[M+Na]^+$ 437.2447, calcd for $[C_{11}H_{25}N_4]^+$ 213.2074 found $[M+H\text{-}HPOPh_2]^+$ 213.2079, calcd. for $[C_{12}H_{12}OP]^+$ 203.0620 found [M-**cyclam**]$^+$ 203.0622

***Synthesis of [Cu(te1po^{Ph})](ClO$_4$)$_2$*:** The pH of a solution of **te1po^{Ph}** (25.0 mg, 0.045 mmol) in H_2O (1.80 mL) was adjusted to 6 using few drops of KOH (0.10 or 0.50 M). Then $Cu(ClO_4)_2.6H_2O$ (17.4 mg, 0.047 mmol) was added to the reaction and the pH drops to 1. The pH was adjusted again to 6 with few drops of KOH (0.10 or 0.5 M). The reaction was stirred under reflux for 18 h. After cooling to room temperature, the solvent was removed under reduced pressure and the complex was purified by C_{18}-Aq flash chromatography (100:0 to 0:100 H_2O/MeOH) to afford the title compound as a purple powder (18.4 mg, 60%). *ESI-HR-MS* (positive, H_2O) *m/z* calcd. for $[C_{23}H_{35}CuN_4OP]^{2+}$ 238.5917 found $[M]^{2+}$ 238.5917, calcd. for $[C_{23}H_{34}CuN_4OP]^+$ 476.1760 found $[M\text{-}H]^+$476.1749, calcd. for $[C_{23}H_{35}ClCuN_4OP]^+$ 512.1527 found $[M+Cl]^+$ 512.1520.

Synthesis of 2: Under nitrogen, diboc-cyclam (1.000 g, 2.50 mmol), diphenylphosphine oxide (1.009 g, 4.99 mmol) and paraformaldehyde (0.150 g, 4.99 mmol) were solubilized in dry CH_3CN (5 mL). The reaction was stirred at 80°C for 3h. Solvents were removed in vacuo. The crude product was purified by column chromatography on silica gel (EA → EA/MeOH 90/10) to give **2** as a white foam (1.199 g, 58%). *^{1}H NMR* ($CDCl_3$, 400 MHz, 298 K, TMS) δ (ppm): 7.85-7.65 (m, 8H, CH_{Ar}), 7.55-7.39 (m, 12H, CH_{Ar}), 3.34 (s, 4H, N-CH_2-PO), 3.08-2.87 (m, 8H, C$H_2\alpha$N), 2.84-2.41 (m, 8H, C$H_2\alpha$N), 1.52 (s, 4H, C$H_2\beta$N), 1.42 (s, 18H, CH_3-Boc). *^{13}C NMR* (CD_3CN, 125 MHz, 343 K, TMS) δ (ppm) 156.7 (*C*O-Boc), 134.9 (d, C_{ipso}, $^1J_{C-P}$ = 94.4 Hz), 132.2 (d, *C*H$_{Ar}$, $^2J_{C-P}$ = 8.8 Hz), 129.8 (d, *C*H$_{Ar}$, $^3J_{C-P}$ = 11.3 Hz), 80.0 (C_{sp}-Boc), [57.2, 56.5, 55.7, 55.6, 55.0, 55.0, 47.1, 46.9] (*C*H$_2\alpha$N), 29.0 (*C*H$_3$-Boc), 27.6 (*C*H$_2\beta$N). *^{31}P NMR* ($CDCl_3$, 162 MHz, 298 K, H_3PO_4) δ (ppm) 29.1 (*P*=O). *ESI-HR-MS* (positive, H_2O) *m/z* calcd. for $[C_{46}H_{63}N_4O_6P_2]^+$ 829.4217 found $[M+H]^+$ 829.4212, calcd. for $[C_{46}H_{62}N_4NaO_6P_2]^+$ 851.4037 found $[M+Na]^+$ 851.4034, calcd. for $[C_{36}H_{48}N_4O_2P_2]^{2+}$ 315.1621 found $[M+2H\text{-}2Boc]^{2+}$ 315.1620, calcd. for $[C_{12}H_{12}OP]^+$ 203.0620 found [M-**cyclam**]$^+$ 203.06.

Synthesis of te2po^{Ph}:* 2** (0.772 g, 0.93 mmol) was dissolved in dichloromethane (6.5 mL) and trifluoroacetic acid (6.5 mL) was added at 0°C. The resulting mixture was stirred for 4 h. The reaction mixture was concentrated in vacuo, dissolved in NaOH (4M) and extracted with CH_2Cl_2 (4 x 30 mL). The organic phase was dried over $MgSO_4$, filtered, and concentrated. The product was dissolved with minimal HCl (3M), then acetone was added, and the mixture was filtered by cannula to afford compound ***te2po^{Ph} as a white powder (0.293 g, 45 %). *^{1}H NMR* (MeOD, 500 MHz, 328 K, TMS) δ (ppm) 7.89 (t, 8H, CH_{Ar}), 7.70-7.58 (m, 12H, CH_{Ar}), 3.76 (s, 4H, N-CH_2-PO), 3.10 (br, 4H, C$H_2\alpha$N), 2.85 (br, 4H, C$H_2\alpha$N), 2.74 (br, 4H, C$H_2\alpha$N), 1.74 (br, 4H, C$H_2\alpha$N), 1.28 (s, 4H, C$H_2\beta$N). *^{13}C NMR* (MeOD, 125 MHz, 328 K, TMS) δ (ppm) 134.4 (*CH*$_{Ar}$), 132.4 (d, *CH*$_{Ar}$, J_{C-P} = 9.0 Hz), 131.5 (d, C_{ipso}, $^1J_{C-P}$ = 95.3 Hz), 130.5 (d, *C*H$_{Ar}$, J_{C-P} = 12.6 Hz), 57.3(*C*H$_2\alpha$N), 53.9 (d, *C*H$_2\alpha$N, $^1J_{C-P}$ = 88.9 Hz), 43.7 (*C*H$_2\alpha$N), 25.7 (*C*H$_2\beta$N). *^{31}P NMR* ($CDCl_3$, 202 MHz, 328 K, H_3PO_4) δ (ppm) 34.4 (*P*=O). *ESI-HR-MS* (positive, H_2O) *m/z* calcd. For $[C_{36}H_{47}N_4O_2P_2]$ 629.3169 found $[M+H]^+$ 629.3169, calcd. for $[C_{36}H_{48}N_4O_2P_2]^{2+}$ 315.1620 found $[M+2H]^{2+}$ 315.1625

Synthesis of [Cu(te2po^{Ph})](ClO$_4$)$_2$* : *te2po^{Ph} was dissolved in aqueous NaOH (1M) and extracted with dichloromethane (31.2 mg, 0.049 mmol). Solvent was removed under vacuum and the solid residue was dissolved in ACN (2 mL) and $Cu(ClO_4)_2.6H_2O$ (19.3 mg, 0.052 mmol) was added. The mixture was stirred under reflux for 18 h. The filtrate was isolated by cannula and the solvent was removed under reduced pressure. Title compound was isolated as a blue powder (33.4 mg, 77%). *ESI-HR-MS* (positive, H_2O) *m/z* calcd. for $[C_{36}H_{46}CuN_4O_2P_2]^{2+}$ 345.6191 found $[M]^{2+}$ 345.6197, calcd. for $[C_{36}H_{45}CuN_4O_2P_2]^+$

690.2308 found $[M-H]^+$690.2308, calcd. for $[C_{36}H_{46}ClCuN_4O_2P_2]^+$ 726.2075 found $[M+Cl]^+$ 726.2073

Author Contributions

The manuscript was written through contributions of all authors. All authors have given approval to the final version of the manuscript.

Associated Content

The Supporting Information is available free of charge at https://pubs.acs.org/doi/10.1021/acs.inorgchem.xxxxxxxxx and contains data for 1H, 13C, and 31P NMR, ESI-HRMS, EPR, X-Ray diffraction measurements for ligands and corresponding complexes; and figures for physico-chemical experiments (kinetic inertness, competition UV-Vis experiments).

Author Information

Corresponding Authors
*Dr. Thibault Troadec, thibault.troadec@univ-brest.fr
*Pr. Raphaël Tripier, raphael.tripier@univ-brest.fr

ORCID

Marie M. Le Roy : 0000-0003-1063-4050

Simon Héry : 0000-0003-3163-7138

Nathalie Saffon-Merceron : 0000-0002-0301-4163

Carlos Platas-Iglesias : 0000-0002-6989-9654

Thibault Troadec : 0000-0002-8005-4302

Raphaël Tripier : 0000-0001-9364-788X

Notes

The authors declare no competing financial interest

Acknowledgements

M.L.R., T.T., and R.T. are grateful to the Région Bretagne and La Ligue contre le Cancer for financial support.

References

(1) Chopra, T.; Sasan, S.; Devi, L.; Parkesh, R.; Kapoor, K. K. A Comprehensive Review on Recent Advances in Copper Sensors. *Coordination Chemistry Reviews* **2022**, *470*, 214704.

(2) Lee, H.; Wu, X.; Sun, L. Copper-Based Homogeneous and Heterogeneous Catalysts for Electrochemical Water Oxidation. *Nanoscale* **2020**, *12* (7), 4187–4218.

(3) McCann, S. D.; Stahl, S. S. Copper-Catalyzed Aerobic Oxidations of Organic Molecules: Pathways for Two-Electron Oxidation with a Four-Electron Oxidant and a One-Electron Redox-Active Catalyst. *Acc. Chem. Res.* **2015**, *48* (6), 1756–1766.

(4) Boros, E.; Packard, A. B. Radioactive Transition Metals for Imaging and Therapy. *Chem. Rev.* **2019**, *119* (2), 870–901.

(5) Price, E. W.; Orvig, C. Matching Chelators to Radiometals for Radiopharmaceuticals. *Chem. Soc. Rev.* **2013**, *43* (1), 260–290.

(6) Denoyer, D.; Clatworthy, S. A.; Cater, M. A. Copper Complexes in Cancer Therapy. *Metallo-drugs: development and action of anticancer agents* **2018**, 469–506.

(7) Atrián-Blasco, E.; Conte-Daban, A.; Hureau, C. Mutual Interference of Cu and Zn Ions in Alzheimer's Disease: Perspectives at the Molecular Level. *Dalton Trans.* **2017**, *46* (38), 12750–12759.

(8) Martell, A. E.; Hancock, R. D.; Motekaitis, R. J. Factors Affecting Stabilities of Chelate, Macrocyclic and Macrobicyclic Complexes in Solution. *Coordination Chemistry Reviews* **1994**, *133*, 39–65.

(9) Pearson, R. G. Hard and Soft Acids and Bases, HSAB, Part 1: Fundamental Principles. *J. Chem. Educ.* **1968**, *45* (9), 581.

(10) Martell, A. E.; Motekaitis, R. J.; Clarke, E. T.; Delgado, R.; Sun, Y.; Ma, R. Stability Constants of Metal Complexes of Macrocyclic Ligands with Pendant Donor Groups. *Supramolecular Chemistry* **1996**, *6* (3–4), 353–363.

(11) Pandya, D. N.; Kim, J. Y.; Park, J. C.; Lee, H.; Phapale, P. B.; Kwak, W.; Choi, T. H.; Cheon, G. J.; Yoon, Y.-R.; Yoo, J. Revival of TE2A; a Better Chelate for Cu(II) Ions than TETA? *Chem. Commun.* **2010**, *46* (20), 3517–3519.

(12) Bass, L. A.; Wang, M.; Welch, M. J.; Anderson, C. J. In Vivo Transchelation of Copper-64 from TETA-Octreotide to Superoxide Dismutase in Rat Liver. *Bioconjugate Chem.* **2000**, *11* (4), 527–532.

(13) Kotek, J.; Lubal, P.; Hermann, P.; Císařová, I.; Lukeš, I.; Godula, T.; Svobodová, I.; Táborský, P.; Havel, J. High Thermodynamic Stability and Extraordinary Kinetic Inertness of Copper(II) Complexes with 1,4,8,11-Tetraazacyclotetradecane-1,8-Bis(Methylphosphonic Acid): Example of a Rare Isomerism between Kinetically Inert Penta- and Hexacoordinated Copper(II) Complexes. *Chemistry – A European Journal* **2003**, *9* (1), 233–248.

(14) Füzerová, S.; Kotek, J.; Císařová, I.; Hermann, P.; Binnemans, K.; Lukeš, I. Cyclam (1,4,8,11-Tetraazacyclotetradecane) with One Methylphosphonate Pendant Arm: A New Ligand for Selective Copper(II) Binding. *Dalton Trans.* **2005**, No. 17, 2908–2915.

(15) Lima, L. M. P.; Esteban-Gómez, D.; Delgado, R.; Platas-Iglesias, C.; Tripier, R. Monopicolinate Cyclen and Cyclam Derivatives for Stable Copper(II) Complexation. *Inorg. Chem.* **2012**, *51* (12), 6916–6927.

(16) Frindel, M.; Camus, N.; Rauscher, A.; Bourgeois, M.; Alliot, C.; Barré, L.; Gestin, J.-F.; Tripier, R.; Faivre-Chauvet, A. Radiolabeling of HTE1PA: A New Monopicolinate Cyclam Derivative for Cu-64 Phenotypic Imaging. In Vitro and in Vivo Stability Studies in Mice. *Nuclear Medicine and Biology* **2014**, *41*, e49–e57.

(17) Conte-Daban, A.; Beyler, M.; Tripier, R.; Hureau, C. Kinetics Are Crucial When Targeting Copper Ions to Fight Alzheimer's Disease: An Illustration with Azamacrocyclic Ligands. *Chemistry – A European Journal* **2018**, *24* (33), 8447–8452.

(18) Knighton, R. C.; Troadec, T.; Mazan, V.; Le Saëc, P.; Marionneau-Lambot, S.; Le Bihan, T.; Saffon-Merceron, N.; Le Bris, N.; Chérel, M.; Faivre-Chauvet, A.; Elhabiri, M.; Charbonnière, L. J.; Tripier, R. Cyclam-Based Chelators Bearing Phosphonated Pyridine Pendants for 64Cu-PET Imaging: Synthesis, Physicochemical Studies, Radiolabeling, and Bioimaging. *Inorg. Chem.* **2021**, *60* (4), 2634–2648.

(19) Carter, K. P.; Young, A. M.; Palmer, A. E. Fluorescent Sensors for Measuring Metal Ions in Living Systems. *Chem. Rev.* **2014**, *114* (8), 4564–4601.
(20) Rakshit, A.; Khatua, K.; Shanbhag, V.; Comba, P.; Datta, A. Cu2+ Selective Chelators Relieve Copper-Induced Oxidative Stress in Vivo. *Chem. Sci.* **2018**, *9* (41), 7916–7930.
(21) Devonport, J.; Bodnár, N.; McGown, A.; Bukar Maina, M.; Serpell, L. C.; Kállay, C.; Spencer, J.; Kostakis, G. E. Salpyran: A Cu(II) Selective Chelator with Therapeutic Potential. *Inorg. Chem.* **2021**, *60* (20), 15310–15320.
(22) Robert, A.; Liu, Y.; Nguyen, M.; Meunier, B. Regulation of Copper and Iron Homeostasis by Metal Chelators: A Possible Chemotherapy for Alzheimer's Disease. *Acc. Chem. Res.* **2015**, *48* (5), 1332–1339.
(23) Esmieu, C.; Guettas, D.; Conte-Daban, A.; Sabater, L.; Faller, P.; Hureau, C. Copper-Targeting Approaches in Alzheimer's Disease: How To Improve the Fallouts Obtained from in Vitro Studies. *Inorg. Chem.* **2019**, *58* (20), 13509–13527.
(24) Atkinson, R. C. J.; Gibson, V. C.; Long, N. J.; White, A. J. P. Coordination Chemistry with Phosphine and Phosphine Oxide-Substituted Hydroxyferrocenes. *Dalton Trans.* **2010**, *39* (32), 7540–7546.
(25) Fawcett, J.; Platt, A. W. G.; Russell, D. R. Structures and Catalytic Properties of Triphenylphosphine Oxide Complexes of Scandium and Lanthanide Triflates. *Polyhedron* **2002**, *21* (3), 287–293.
(26) Platt, A. W. G. Lanthanide Phosphine Oxide Complexes. *Coordination Chemistry Reviews* **2017**, *340*, 62–78.
(27) Tsai, W.; Liu, Y.-H.; Peng, S.-M.; Liu, S.-T. Structural Characterization and Catalytic Activities of Copper Complexes with Pyridine-Amine-Phosphine-Oxide Ligand. *Journal of Organometallic Chemistry* **2005**, *690* (2), 415–421.
(28) Hung-Low, F.; Klausmeyer, K. K. Syntheses and Coordination Chemistry of Methylpyridylphosphine Oxide Ligands with Copper(II). *Polyhedron* **2010**, *29* (6), 1676–1686.
(29) Kochel, A. Synthesis and Magnetic Properties of the Copper(II) Complex Derived from Dimethyl Aminomethylphosphine Oxide Ligand. X-Ray Crystal Structure of DMAO and [Cu(NO3)2(POC3H10N)2]. *Inorganica Chimica Acta* **2009**, *362* (4), 1379–1382.
(30) Aleksanyan, D. V.; Nelyubina, Y. V.; Dmitrienko, A. O.; Bushmarinov, I. S.; Klemenkova, Z. S.; Kozlov, V. A. Coordination Diversity of Copper(II) Phosphoryl-Functionalized Salicylaldiminates: Effect of the Length of the Pendant Phosphoryl Arm. *Polyhedron* **2015**, *85*, 295–301.
(31) Sinyavskaya, É. I.; Tsymbal, L. V.; Yatsimirskii, K. B.; Pisareva, S. A.; Medved, T. Ya.; Kabachnik, M. I. Reaction of Alkali-Metal 2,4-Dinitrophenolates with 1,4,7,10-Tetra(Diphenylphosphinylethyl)-1,4,7,10-Tetraazacyclododecane. *Russ Chem Bull* **1986**, *35* (1), 160–165.
(32) Tsebrikova, G. S.; Polyakova, I. N.; Solov'ev, V. P.; Ivanova, I. S.; Kalashnikova, I. P.; Kodina, G. E.; Baulin, V. E.; Tsivadze, A. Yu. Complexation of the New Tetrakis[Methyl(Diphenylphosphorylated)] Cyclen Derivative with Transition Metals: First Examples of Octacoordinate Zinc(II) and Cobalt(II) Complexes with Cyclen Molecules. *Inorganica Chimica Acta* **2018**, *478*, 250–259.
(33) Herrero, C.; Quaranta, A.; Ghachtouli, S. E.; Vauzeilles, B.; Leibl, W.; Aukauloo, A. Carbon Dioxide Reduction via Light Activation of a Ruthenium–Ni(Cyclam) Complex. *Phys. Chem. Chem. Phys.* **2014**, *16* (24), 12067–12072.
(34) Royal, G.; Dahaoui-Gindrey, V.; Dahaoui, S.; Tabard, A.; Guilard, R.; Pullumbi, P.; Lecomte, C. New Synthesis of Trans-Disubstituted Cyclam Macrocycles – Elucidation of the Disubstitution Mechanism on the Basis of X-Ray Data and Molecular Modeling. *European Journal of Organic Chemistry* **1998**, *1998* (9), 1971–1975.
(35) Keglevich, G.; Bálint, E. The Kabachnik–Fields Reaction: Mechanism and Synthetic Use. *Molecules* **2012**, *17* (11), 12821–12835.
(36) Bosnich, B.; Tobe, M. L.; Webb, G. A. Complexes of Nickel(II)with a Cyclic Tetradentate Secondary Amine. *Inorg. Chem.* **1965**, *4* (8), 1109–1112.
(37) Whimp, P. O.; Bailey, M. F.; Curtis, N. F. Some Cyclic Tetra-Amines and Their Metal-Ion Complexes. Part VI. The Crystal Structure of Acetato-C-Rac-(5,7,7,12,14,14-Hexamethyl-1,4,8,11-Tetra-Azacyclotetradecane)Nickel(II) Perchlorate. *J. Chem. Soc. A* **1970**, No. 0, 1956–1963.
(38) Gilheany, D. G. No d Orbitals but Walsh Diagrams and Maybe Banana Bonds: Chemical Bonding in Phosphines, Phosphine Oxides, and Phosphonium Ylides. *Chem. Rev.* **1994**, *94* (5), 1339–1374.
(39) Dobado, J. A.; Martínez-García, H.; Molina; Sundberg, M. R. Chemical Bonding in Hypervalent Molecules Revised. Application of the Atoms in Molecules Theory to Y3 X and Y3 XZ (Y = H or CH3; X = N, P or As; Z = O or S) Compounds. *J. Am. Chem. Soc.* **1998**, *120* (33), 8461–8471.
(40) Stoll, S.; Schweiger, A. EasySpin, a Comprehensive Software Package for Spectral Simulation and Analysis in EPR. *Journal of Magnetic Resonance* **2006**, *178* (1), 42–55.
(41) Molton, F. Simultispin: A Versatile Graphical User Interface for the Simulation of Solid-State Continuous Wave EPR Spectra. *Magnetic Resonance in Chemistry* **2020**, *58* (8), 718–726.
(42) AlHaddad, N.; Lelong, E.; Suh, J.-M.; Cordier, M.; Lim, M. H.; Royal, G.; Platas-Iglesias, C.; Bernard, H.; Tripier, R. Copper(II) and Zinc(II) Complexation with N-Ethylene Hydroxycyclams and Consequences on the Macrocyclic Backbone Configuration. *Dalton Trans.* **2022**, *51* (22), 8640–8656.
(43) Kossmann, S.; Kirchner, B.; Neese, F. Performance of Modern Density Functional Theory for the Prediction of Hyperfine Structure: Meta-GGA and Double Hybrid Functionals. *Mol. Phys.* **2007**, *105* (15–16), 2049–2071.
(44) Drosou, M.; Mitsopoulou, C. A.; Orio, M.; Pantazis, D. A. EPR Spectroscopy of Cu(II) Complexes: Prediction of g-Tensors Using Double-Hybrid Density Functional Theory. *Magnetochemistry* **2022**, *8* (4), 36.
(45) Hancock, R. D.; Motekaitis, R. J.; Mashishi, J.; Cukrowski, I.; Reibenspies, J. H.; Martell, A. E. The Unusual Protonation Constants of Cyclam. A Potentiometric, Crystallographic and Molecular Mechanics Study. *J. Chem. Soc., Perkin Trans. 2* **1996**, No. 9, 1925–1929.
(46) Rahardjo, S. B.; Wainwright, K. P. Hydroxyethylation and Its Effect on the Rate of Metal Ion Ingress into Macrocyclic Ligands. *Inorg. Chim. Acta* **1997**, *255* (1), 29–34.
(47) Frindel, M.; Saëc, P. L.; Beyler, M.; Navarro, A.-S.; Saï-Maurel, C.; Alliot, C.; Chérel, M.; Gestin, J.-F.; Faivre-Chauvet, A.; Tripier, R. Cyclam Te1pa for 64Cu PET Imaging. Bioconjugation to Antibody, Radiolabeling and Preclinical Application in Xenografted Colorectal Cancer. *RSC Adv.* **2017**, *7* (15), 9272–9283.
(48) Hathaway, B. J.; Billing, D. E. The Electronic Properties and Stereochemistry of Mono-Nuclear Complexes of the

Copper(II) Ion. *Coordination Chemistry Reviews* **1970**, *5* (2), 143–207.

(49) Regueiro-Figueroa, M.; Lima, L. M. P.; Blanco, V.; Esteban-Gómez, D.; de Blas, A.; Rodríguez-Blas, T.; Delgado, R.; Platas-Iglesias, C. Reasons behind the Relative Abundances of Heptacoordinate Complexes along the Late First-Row Transition Metal Series. *Inorg. Chem.* **2014**, *53* (24), 12859–12869.

(50) Markham, G. D.; Glusker, J. P.; Bock, C. W. The Arrangement of First- and Second-Sphere Water Molecules in Divalent Magnesium Complexes: Results from Molecular Orbital and Density Functional Theory and from Structural Crystallography. *J. Phys. Chem. B* **2002**, *106* (19), 5118–5134.

(51) Bock, C. W.; Markham, G. D.; Katz, A. K.; Glusker, J. P. The Arrangement of First- and Second-Shell Water Molecules Around Metal Ions: Effects of Charge and Size. *Theor. Chem. Acc.* **2006**, *115* (2), 100–112.

(52) Regueiro-Figueroa, M.; Esteban-Gómez, D.; Pujales-Paradela, R.; Caneda-Martínez, L.; de Blas, A.; Platas-Iglesias, C. Water Exchange Rates and Mechanisms in Tetrahedral [Be(H2O)4]2+ and [Li(H2O)4]+ Complexes Using DFT Methods and Cluster-Continuum Models. *Int. J. Quantum Chem.* **2016**, *116* (19), 1388–1396.

(53) Stoll, S.; Schweiger, A. EasySpin, a Comprehensive Software Package for Spectral Simulation and Analysis in EPR. *Journal of Magnetic Resonance* **2006**, *178* (1), 42–55.

(54) Molton, F. Simultispin: A Versatile Graphical User Interface for the Simulation of Solid-State Continuous Wave EPR Spectra. *Magn Reson Chem* **2020**, *58* (8), 718–726.

(55) Sheldrick, G. M. SHELXT – Integrated Space-Group and Crystal-Structure Determination. *Acta Cryst A* **2015**, *71* (1), 3–8.

(56) Sheldrick, G. M. Crystal Structure Refinement with SHELXL. *Acta Cryst C* **2015**, *71* (1), 3–8.

(57) Spek, A. L. PLATON SQUEEZE: A Tool for the Calculation of the Disordered Solvent Contribution to the Calculated Structure Factors. *Acta Cryst C* **2015**, *71* (1), 9–18.

(58) Frisch, M. J.; Trucks, G. W.; Schlegel, H. B.; Scuseria, G. E.; Robb, M. A.; Cheeseman, J. R.; Scalmani, G.; Barone, V.; Petersson, G. A.; Nakatsuji, H. Gaussian 16; Gaussian, Inc., Wallingford, CT, 2016.

(59) Chai, J.-D.; Head-Gordon, M. Long-Range Corrected Hybrid Density Functionals with Damped Atom–Atom Dispersion Corrections. *Phys. Chem. Chem. Phys.* **2008**, *10* (44), 6615–6620.

(60) Weigend, F.; Ahlrichs, R. Balanced Basis Sets of Split Valence, Triple Zeta Valence and Quadruple Zeta Valence Quality for H to Rn: Design and Assessment of Accuracy. *Phys. Chem. Chem. Phys.* **2005**, *7* (18), 3297–3305.

(61) Tomasi, J.; Mennucci, B.; Cammi, R. Quantum Mechanical Continuum Solvation Models. *Chem. Rev.* **2005**, *105* (8), 2999–3094.

(62) Neese, F. The ORCA Program System. *WIREs Computational Molecular Science* **2012**, *2* (1), 73–78.

(63) Neese, F. Software Update: The ORCA Program System, Version 4.0. *WIREs Computational Molecular Science* **2018**, *8* (1), e1327.

(64) Tao, J.; Perdew, J. P.; Staroverov, V. N.; Scuseria, G. E. Climbing the Density Functional Ladder: Nonempirical Meta--Generalized Gradient Approximation Designed for Molecules and Solids. *Phys. Rev. Lett.* **2003**, *91* (14), 146401.

(65) Brémond, E.; Adamo, C. Seeking for Parameter-Free Double-Hybrid Functionals: The PBE0-DH Model. *J. Chem. Phys.* **2011**, *135* (2), 024106.

(66) Lenthe, E. van; Baerends, E. J.; Snijders, J. G. Relativistic Regular Two-component Hamiltonians. *J. Chem. Phys.* **1993**, *99* (6), 4597–4610.

(67) van Lenthe, E.; Baerends, E. J.; Snijders, J. G. Relativistic Total Energy Using Regular Approximations. *J. Chem. Phys.* **1994**, *101* (11), 9783–9792.

(68) Pantazis, D. A.; Chen, X.-Y.; Landis, C. R.; Neese, F. All-Electron Scalar Relativistic Basis Sets for Third-Row Transition Metal Atoms. *J. Chem. Theory Comput.* **2008**, *4* (6), 908–919.

(69) Neese, F.; Wennmohs, F.; Hansen, A.; Becker, U. Efficient, Approximate and Parallel Hartree–Fock and Hybrid DFT Calculations. A 'Chain-of-Spheres' Algorithm for the Hartree–Fock Exchange. *Chem. Phys.* **2009**, *356* (1), 98–109.

(70) Stoychev, G. L.; Auer, A. A.; Neese, F. Automatic Generation of Auxiliary Basis Sets. *J. Chem. Theory Comput.* **2017**, *13* (2), 554–562.

(71) Heß, B. A.; Marian, C. M.; Wahlgren, U.; Gropen, O. A Mean-Field Spin-Orbit Method Applicable to Correlated Wavefunctions. *Chemical Physics Letters* **1996**, *251* (5), 365–371.

(72) Neese, F. Efficient and Accurate Approximations to the Molecular Spin-Orbit Coupling Operator and Their Use in Molecular g-Tensor Calculations. *J. Chem. Phys.* **2005**, *122* (3), 034107.

(73) Marenich, A. V.; Cramer, C. J.; Truhlar, D. G. Universal Solvation Model Based on Solute Electron Density and on a Continuum Model of the Solvent Defined by the Bulk Dielectric Constant and Atomic Surface Tensions. *J. Phys. Chem. B* **2009**, *113* (18), 6378–6396.

(74) Gans, P.; O'Sullivan, B. GLEE, a New Computer Program for Glass Electrode Calibration. *Talanta* **2000**, 51 (1), 33–37.

(75) Gans, P.; Sabatini, A.; Vacca, A. Investigation of Equilibria in Solution. Determination of Equilibrium Constants with the HYPERQUAD Suite of Programs. *Talanta* **1996**, 43 (10), 1739–1753.

(76) Gampp, H.; Maeder, M.; Meyer, C. J.; Zuberbühler, A. D. Calculation of Equilibrium Constants from Multiwavelength Spectroscopic Data—IMathematical Considerations. *Talanta* **1985**, *32* (2), 95–101.

Graphical TOC

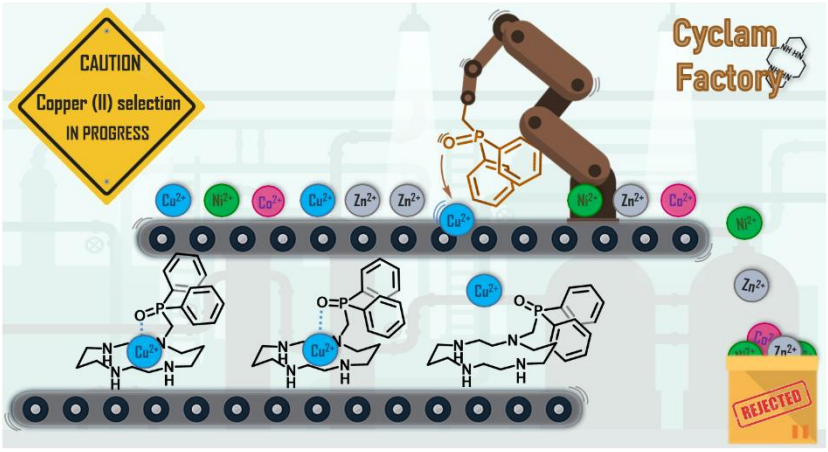

Phosphine oxide makes the selection: A new phosphine oxide-appended cyclam ligand has been prepared, demonstrating exceptional selectivity for Cu^{2+} cations over other divalent zinc, nickel and cobalt congeners, as demonstrated through competition experiments in UV-Vis spectroscopy and confirmed by DFT calculations.